

## Photoproduction and Quenching of Hydrated Electrons from Dissolved Organic Matter in Natural Waters

Yu-ichiro KUMAMOTO, Jian WANG, and Kitao FUJIWARA\*

School of Biosphere Sciences, Hiroshima University, Kagamiyama 1-7-1, Higashi-Hiroshima 724

(Received September 13, 1993)

Laser photolysis was used to investigate the production and quenching of hydrated electrons formed after absorption of 355 nm light by dissolved organic matter (DOM) in natural waters. Correlation between the hydrated electrons generated and dissolved organic carbon in seawaters was found. The DOM in land waters ejected more hydrated electrons than seawater DOM did. Land waters contained much natural fluorescent organic matter, so the DOM in the land waters was rich in photochemically sensitive chromophores. Quenching of the hydrated electrons by the inorganic ions, nitrite, nitrate,  $\text{Cd}^{2+}$ ,  $\text{Ni}^{2+}$ ,  $\text{Co}^{2+}$ , and  $[\text{Co}(\text{NH}_3)_6]^{3+}$  were investigated by a first-order function and the Stern–Volmer model. With the former, the quenching rate constants were  $10^{-9}$  to  $10^{-10} \text{ dm}^3 \text{ mol}^{-1} \text{ s}^{-1}$ , which was close to reported values. No regional differences were found among the seawater samples. This result suggested similar quenching mechanisms for hydrated electrons generated in the different seawaters. With the Stern–Volmer model, primary quenching was estimated. Quenching studies of land waters suggested that DOM had an aggregate nature in such waters.

A number of studies on photochemical reactions in aqueous systems have been reported in the past decade.<sup>1–3)</sup> The photolysis of many defined chromophores have been investigated under natural aquatic conditions, but little is known about the structures and characteristics of natural organic compounds during photolysis. Such substances, including humic substances (HUS), are important in aquatic ecosystems.<sup>4–6)</sup>

Laser radiation has been used in flash photolysis of aqueous solutions of HUS.<sup>7–12)</sup> In these laser studies, it is possible to observe the absorption spectra and the decay of transient species that mediate the sensitized photoprocesses. These studies have provided evidence that HUS from natural soils and waters produce hydrated electrons on absorption of near-ultraviolet light. These findings confirmed earlier speculations that hydrated electrons could be produced photochemically from polyhydroxy aromatic compounds,<sup>13,14)</sup> which are structural components of HUS.<sup>4)</sup>

The formation of hydrated electrons in natural waters is the first step in a series of photochemical reactions. Hydrated electrons react rapidly with organic and inorganic species that contain electronegative atoms. In natural waters, the hydrated electrons generated react with dissolved oxygen and  $\text{H}^+$  at a diffusion-controlled rate, resulting in the formation of hydrogen peroxide.<sup>15–17)</sup> Studies of quenching the hydrated electrons by coexistent substances gives information about the initiation of photochemical reactions, which is related to the characteristics of dissolved organic matter (DOM), including HUS, in natural waters.

In this study, we investigate the photoproduction of hydrated electrons and their quenching by anions and cations in various natural waters. Our purpose is to describe the photochemical characteristics of DOM in natural waters.

### Experimental

**Samples.** Surface seawater was collected in coastal and open ocean at the sampling points shown in Fig. 1. The sample of Hiroshima Bay (station A) was collected with a polyethylene container from the shore and transferred to a polyethylene bottle. It was immediately filtered through an ignited (1 h at 450 °C) glass-fiber filter (Advantec GC-50; 0.5- $\mu\text{m}$  pores) and stored in a freezer until analysis. Sampling in the Pacific Ocean (stations B, C, and D) was done during a cruise of research vessels Tansei Maru and Hakuho Maru of the Ocean Research Institute, University of Tokyo. At stations C and D, sampling was done 4 times with about 6 h intervening each time. All samples from the Pacific Ocean were frozen immediately. In the laboratory, they were melted at room temperature, filtered, and stored in a freezer. Land waters were collected from marches (Okuda and Budo Ponds) and the Kurose River near Hiroshima University in Higashi-Hiroshima City. The water was filtered and stored as the seawaters were.

Humic acid solution was prepared by extraction of 1 g of a commercial preparation (Wako Pure Chemical Industries) with 1 L ( $\text{L}=\text{dm}^3$ ) of 0.1  $\text{mol L}^{-1}$  sodium hydroxide for 24 h. The solution was filtered with a glass-fiber filter (Advantec GC-50). The filtrate was adjusted to pH 6.0 by the addition of HCl (0.1  $\text{mol L}^{-1}$ ), and the mixture was filtered and stored. It was diluted by distilled water before laser irradiation.

**Laser Photolysis.** Figure 2 is a diagram of the system for observation of the generation of hydrated electrons in samples during laser photolysis. The third harmonic wave (355 nm) of a Nd:YAG laser (Spectra-Physics, GCR-11) was used to irradiate samples in a quartz cell (path length, 10 mm) for ordinary fluorescence spectrometry. The laser output was about 60 mJ per pulse with a duration of 5–6 ns. The hydrated electrons generated were monitored with a laser diode (Sharp, LTO-30MD: 750 nm, 3 mW). The temporal absorption of the laser diode due to the hydrated electrons was detected by a photodiode (Sharp, PD50PI) to which a 9-V current was biased in reverse. The output of the photodiode was fed into a 100-MHz digital storage os-

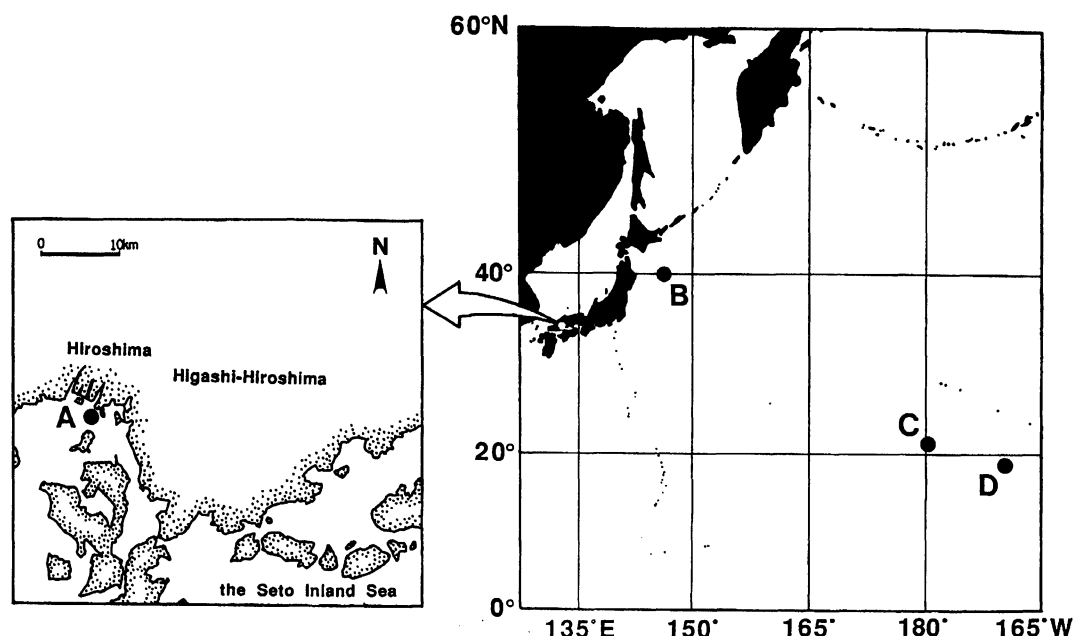


Fig. 1. Sampling locations. Station A: 132°28'E 34°21'N, 1992 Nov. 2, Station B: 146°00'E 40°00'N, 1992 Nov. 17, Station C: 179°51'W 20°59'N, 1993 Feb. 17–18, Station D: 169°00'W 19°20'N, 1993 Feb. 4–5.

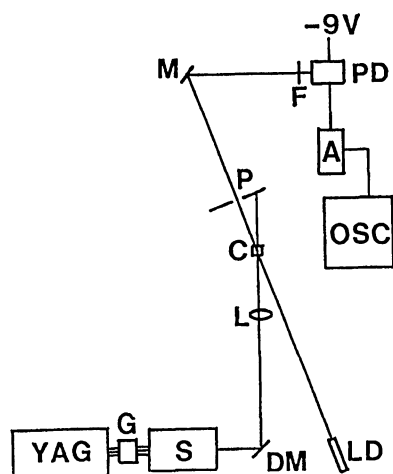


Fig. 2. Optical configuration for laser photolysis to generate hydrated electrons. YAG, YAG laser; G, third harmonic generator; S, wave separator; DM, dichroic mirror; L, convex quartz lens; C, sample container (10-mm quartz cell); P, pin hole; M, mirror; F, low cut filter to eliminate 355-nm YAG laser light; PD, photodiode; A, amplifier; OSC, sampling digital oscilloscope.

cilloscope (Yokogawa, DL1200) through a laboratory-made A/V amplifier. Fifty ohms resistance (Kenwood, TA-57) was applied before the input by the A/V amplifier and the digital storage oscilloscope.

Air-purging with argon (200 mL min<sup>-1</sup>) was done for all of the samples for 10 min just before measurement. An *N,N*-dimethylaniline solution (10 mmol L<sup>-1</sup>) was measured before the samples as the standard of electron generation. For the study of quenching, the samples containing trichloroacetic acid (5 mmol L<sup>-1</sup>) were used as blanks in which the hydrated electrons were completely quenched. When

quenching by metal ions was to be observed, the samples were brought to pH 6.0 with a 0.1 mol L<sup>-1</sup> HCl solution. In the other experiments, the pH of the samples was between 7.2 and 8.2. In the laser photolysis of *N,N*-dimethylaniline, no significant differences were found in the generation of hydrated electrons in the pH range of 6.0 to 8.2. The background concentrations of certain quenchers in the samples were measured in advance of the quenching studies: Metal ions were negligibly low in concentration and nitrite and nitrate were in the range of 0.2–3.9 μmol L<sup>-1</sup>, and this range was used for correction of the amount of the quencher.

**Measurements Other than Photolysis.** Natural fluorescence (fluorescent organic matter) in the samples was measured by a fluorescence spectrophotometer (Hitachi Inc., model 650-10LC). Chen and Bada<sup>18)</sup> showed that any reasonable pair of wavelengths of excitation (300–360 nm) and emission (400–500 nm) could give a representative of the seawater fluorescence spectrum. In this study, the excitation and emission wavelengths were set at 320 and 420 nm (10-nm bandwidth), respectively. Because these wavelengths were different from those used by Kalle,<sup>19)</sup> Dorsch and Bidleman,<sup>20)</sup> and Chen and Bada,<sup>18)</sup> the fluorescence spectrophotometer was adjusted so that 2.8 μg L<sup>-1</sup> quinine sulfate solution at pH 2 gave 25 arbitrary units of fluorescence (flu); the analytical precision of the measurement was ±0.2 flu. Absorption spectra of the samples were measured by a spectrophotometer-220A (Hitachi Inc.). Dissolved organic carbon (DOC) was measured by a TOC-500 apparatus (Shimadzu Corp.). Samples (5 mL) were acidified with 12 mol L<sup>-1</sup> HCl (50 μL) and dissolved inorganic carbon was expelled from the samples by oxygen gas. An aqueous solution of potassium hydrogen phthalate was used to calibrate the infrared analyzer absorption intensity. Standard errors of the DOC measurement were less than 5%.

## Results and Discussion

**Transient Absorption of Hydrated Electrons after Photolysis.** Figure 3A shows a plot of the optical density at 750 nm for the seawater from station A. A short-lived transient absorption with a lifetime ranged between 1.0 and 2.0  $\mu\text{s}$  was found. This absorption was completely quenched by the addition of trichloroacetic acid ( $5.0 \text{ mmol L}^{-1}$ ) or  $1.6 \times 10^{-1} \text{ mol L}^{-1} \text{ H}^+$  (Fig. 3B). Trichloroacetic acid and  $\text{H}^+$  react with hydrated electrons via a diffusion-controlled process.<sup>21)</sup> The quenching by trichloroacetic acid and  $\text{H}^+$  shows that the short-lived transient species was owing to hydrated electrons. The absorption by hydrated electrons was followed by a delayed small transient absorption in Fig. 3B. This absorption was due to radicals, cations of organic matter, and their triplet states, produced after the release of electrons.<sup>7,8,10)</sup> The decay pattern (a fast peak and a delayed small transient absorption) of the optical density was found with all of the seawater samples.

The amount of hydrated electrons generated within 1  $\mu\text{s}$  by laser irradiation was estimated based on the peak height (distance between the highest value and the base line). The net absorption was found by subtraction of the peak height of a sample to which trichloroacetic acid ( $5.0 \text{ mmol L}^{-1}$ ) was added from the peak height of a sample with no addition. Within 1  $\mu\text{s}$ , the transient decay curves fitted the single exponential functions, by which a mean lifetime of hydrated electrons was calculated ( $\text{lifetime} = T_{1/2}/\ln 2$ ; here,  $T_{1/2}$  is the half-life of a hydrated electron). Absorption at time zero was estimated by single exponential functions. The value of the extrapolated absorption agreed with that of the net absorption, so the net absorption probably expressed the true absorption at time zero.

**Generation of Hydrated Electrons in Natural Waters.** Table 1 shows the absorbance and lifetime of generated hydrated electrons as well as pH, DOC, fluorescent organic matter, and absorbance at 355 nm for natural waters and the humic acid solutions. The lifetimes of the hydrated electrons were similar in different seawater samples. With land waters and humic acid solutions, the exact lifetimes could not be obtained because of long-lived transient species, which could be due to the triplet states of DOM produced after the release of electrons.

The generation of hydrated electrons in land waters was greater than in the seawaters. Fluorescent organic matter was abundant in the land waters, so absorbance at the laser irradiation wavelength (355 nm) was large. Figure 4A shows the correlation between the absorbance (peak height) of the hydrated electrons generated and the amount of fluorescent organic matter. The concentration of the fluorescent organic matter is related with photoproduction of hydrated electrons in aquatic systems. Photodegradation of fluorescent organic mat-

ter in surface seawater has been reported,<sup>22–26)</sup> and this phenomenon also suggested that fluorescent organic matter was a photosensitizer that produces hydrated electrons. The seawater of station A had a similar concentration of fluorescent organic matter as the land waters, but the land waters produced more hydrated electrons. This difference suggests that characteristics of the fluorescent organic matter in land water and in seawater are different.

Figure 4B shows correlation between the absorbance (peak height) of hydrated electrons generated and DOC. In seawater, there was correlation between the hydrated electrons generated and DOC ( $r=0.710$ ). Figure 4B also shows differences between seawaters and land waters. Smart et al.<sup>27)</sup> and Laane and Koole<sup>28)</sup> found that DOC and fluorescent organic matter were correlated in various estuarine and coastal waters. We found no correlation between DOC and fluorescent organic matter in these natural samples. The “terrestrial HUS” in the seawater is not the same as that in the land water in terms of photoproduction of hydrated electrons.

With the humic acid solutions, there was correlation between the hydrated electrons generated and the fluorescent organic matter ( $r=0.987$ , Fig. 4A) and DOC ( $r=0.995$ , Fig. 4B). The slope of the line of regression between the hydrated electrons generated and DOC was almost the same with seawater and with the humic acid solutions. This similarity suggests that DOM in the seawaters shared photochemical characteristics with those of humic acid.

**Quenching Studies.** Quenching of the hydrated electrons generated by nitrite ion, nitrate ion,  $\text{Cd}^{2+}$ ,  $\text{Ni}^{2+}$ ,  $\text{Co}^{2+}$ , and  $[\text{Co}(\text{NH}_3)_6]^{3+}$  was investigated. Figure 5 shows the quenching patterns of hydrated electrons in seawater from station A with nitrate as the quencher. If we assume that the quenching of hydrated electrons in aquatic systems obeys the first-order reaction, the concentration of the hydrated electron,  $[\text{E}]$ , at time  $t$  can be given as:

$$[\text{E}] = [\text{E}_0] \exp(-k_{\text{app}}t) = [\text{E}_0] \exp(-k[\text{Q}]t) \quad (1)$$

Here  $k_{\text{app}}$  is the apparent quenching rate constant and  $k$  is the quenching rate constant.  $[\text{E}_0]$  is the concentration of hydrated electron at the time zero.  $[\text{Q}]$  is the concentration of the quencher. The decay patterns in the transient absorption of hydrated electrons observed in the quenching experiment with sample from stations A, B, and C at 18:00 satisfactorily fitted Eq. 1 within 1  $\mu\text{s}$ . Table 2 shows the calculated rate constant,  $k$ . The values of  $k$  were closed to the rate constant observed by a radiolysis methods.<sup>21)</sup> The values of  $k$  were found to decrease in the following order:  $[\text{Co}(\text{NH}_3)_6]^{3+} > \text{NO}_3^- = \text{Cd}^{2+} > \text{NO}_2^- > \text{Ni}^{2+} = \text{Co}^{2+}$ . This order was the same for seawater samples from stations A, B, and C at 18:00, suggesting similar characteristics

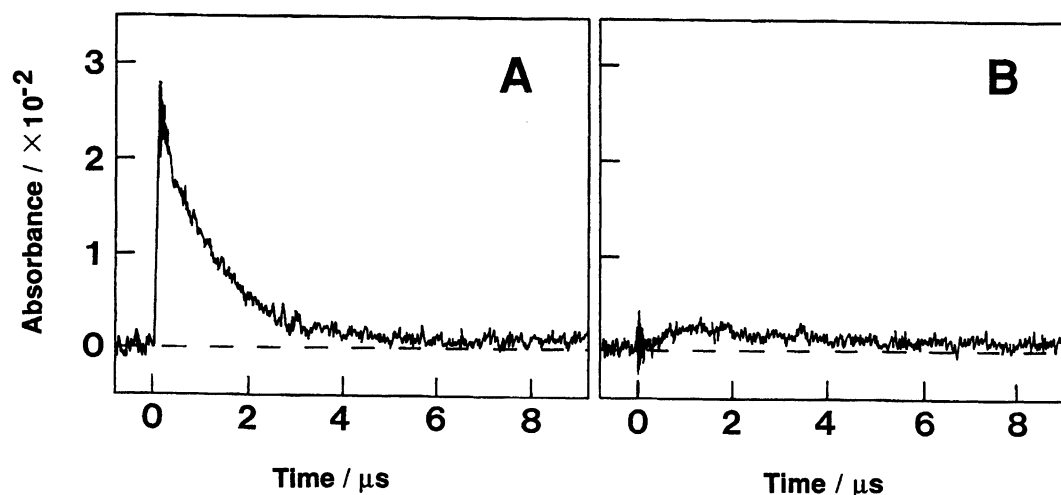


Fig. 3. Decay of the transient absorption ( $\lambda=750$  nm) induced by laser irradiation of seawater from station A: (A) purging of air with argon for 10 min without a quencher (pH 8.2); (B) with trichloroacetic acid ( $5 \text{ mmol L}^{-1}$ ) or with pH adjusted to 0.8 with  $12 \text{ mol L}^{-1}$  HCl (both decay patterns of absorption were same within the experimental error).

Table 1. The Absorbance and Lifetime of the Generated Hydrated Electrons and the Characteristics of the Samples

Sample	pH	Absorbance of the hydrated electrons $\times 10^2$	Lifetime of the hydrated electrons/ $\mu\text{s}$	DOC/ $\text{mg CL}^{-1}$	Fluorescent organic matter/flu.	Absorbance at 355nm $\times 10^3$
St. A	8.0	$2.3 \pm 0.1$	$1.2 \pm 0.4$	$1.7 \pm 0.03$	51	3.5
St. B	8.1	$1.5 \pm 0.1$	$1.4 \pm 0.3$	$0.66 \pm 0.06$	8.0	1.3
St. C 23:00	8.1	$1.4 \pm 0.1$	$1.2 \pm 0.1$	$0.77 \pm 0.13$	4.3	0.4
St. C 07:50	8.1	$2.1 \pm 0.1$	$1.3 \pm 0.3$	$0.97 \pm 0.04$	4.6	0.4
St. C 12:00	8.2	$1.3 \pm 0.1$	$1.6 \pm 0.5$	$0.56 \pm 0.01$	4.1	0.2
St. C 18:00	8.0	$2.2 \pm 0.1$	$1.5 \pm 0.2$	$1.3 \pm 0.03$	5.0	0.4
St. D 24:00	8.1	$2.2 \pm 0.2$	$1.0 \pm 0.1$	$1.1 \pm 0.05$	7.7	0.9
St. D 06:00	8.2	$2.1 \pm 0.1$	$1.2 \pm 0.5$	$1.1 \pm 0.07$	4.8	1.3
St. D 12:00	8.1	$2.6 \pm 0.0$	$1.8 \pm 0.1$	$0.95 \pm 0.02$	4.4	0.1
St. D 18:00	8.1	$2.1 \pm 0.2$	$1.1 \pm 0.2$	$1.0 \pm 0.09$	3.9	0.2
Kurose River	7.6	$9.1 \pm 1.0$	—	$1.3 \pm 0.01$	100	14
Okuda Pond	7.3	$14 \pm 0.6$	—	$1.5 \pm 0.05$	48	14
Budo Pond	7.2	$9.7 \pm 0.7$	—	$1.0 \pm 0.06$	65	10
Humic acid						
1/600 dilution <sup>a)</sup>	6.5	$1.4 \pm 0.1$	—	$0.57 \pm 0.01$	37	18
1/400	6.5	$1.8 \pm 0.1$	—	$0.86 \pm 0.02$	54	31
1/300	6.5	$2.4 \pm 0.1$	—	$1.3 \pm 0.06$	70	41
1/200	6.5	$3.2 \pm 0.1$	—	$1.7 \pm 0.05$	100	63
1/100	6.5	$5.0 \pm 0.2$	—	$3.4 \pm 0.06$	170	120
1/75	6.5	$7.2 \pm 0.2$	—	$4.5 \pm 0.18$	210	160

a) Humic acid solution was diluted with distilled water.

for different (coastal or open ocean) seawaters in terms of the quenching of photochemically produced hydrated electrons. Among anions or cations, the order of  $k$  corresponded with the order of the redox potential;<sup>29)</sup> nitrate, with its higher redox potential, was a stronger than nitrite was. The order of the redox potentials for the cations was:  $[\text{Co}(\text{NH}_3)_6]^{3+} > \text{Ni}^{2+} \approx \text{Co}^{2+} > \text{Cd}^{2+}$ , which was the same as the order of  $k$  except for  $\text{Cd}^{2+}$ .

The Stern-Volmer model<sup>30)</sup> was used to study the quenching of hydrated electrons. Stern-Volmer analysis of photochemical kinetics is possible for two proc-

esses: unimolecular decay and bimolecular quenching of an electronically excited species. The intensity of an electronically excited substance in the absence ( $I_0$ ) and in the presence ( $I$ ) of a quencher (molar concentration,  $[\text{Q}]$ ) are expressed as:

$$I_0/I = \tau_0/\tau = 1 + K_{\text{SV}}[\text{Q}] = 1 + k_{\text{SV}}\tau_0[\text{Q}] \quad (2)$$

Here,  $K_{\text{SV}}$  is the Stern-Volmer constant and is equal to  $k_{\text{SV}}\tau_0$ , where  $k_{\text{SV}}$  is the rate constant for quenching.  $\tau_0$  and  $\tau$  are the lifetimes of the excited substance in the

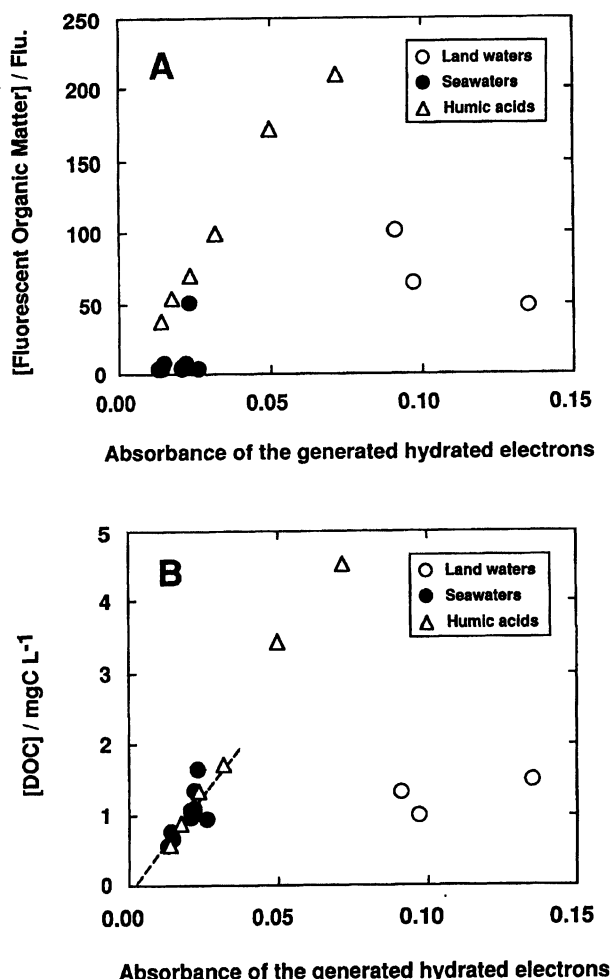


Fig. 4. Correlation between the absorbance (peak height) of the hydrated electrons generated and the fluorescent organic matter (A) or DOC (B) in seawater (●), land water (○), and Humic acid solution (△). Dashed line shows the line of regression for seawater (correlation coefficient  $r=0.710$ ).

absence and the presence of the quencher, respectively.

Figure 6 shows Stern-Volmer plots of seawater from station A when nitrite or nitrate was used as the quencher.  $I_0$  ( $\tau_0$ ) and  $I$  ( $\tau$ ) is absorption intensity (lifetime) of hydrated electrons in the absence and in the presence of a quencher, respectively.  $I_0/I$  and  $\tau_0/\tau$  increase against the concentration of nitrite (or nitrate). From Eq. 2, the Stern-Volmer model for lifetime quenching of hydrated electrons was given as:

$$\tau_0/\tau = 1 + K_{SV}^t[Q] = 1 + k_t\tau_0[Q] \quad (3)$$

Here  $K_{SV}^t$  is the quenching constant for lifetime, where  $k_t$  is the quenching rate constant for lifetime. The values of  $k_t$  were in good agreement with those of  $k$  (Table 2). This agreement suggests that the Stern-Volmer model for lifetime quenching can be applied to the decay of hydrated electrons in natural waters.

The Stern-Volmer model for the intensity quenching

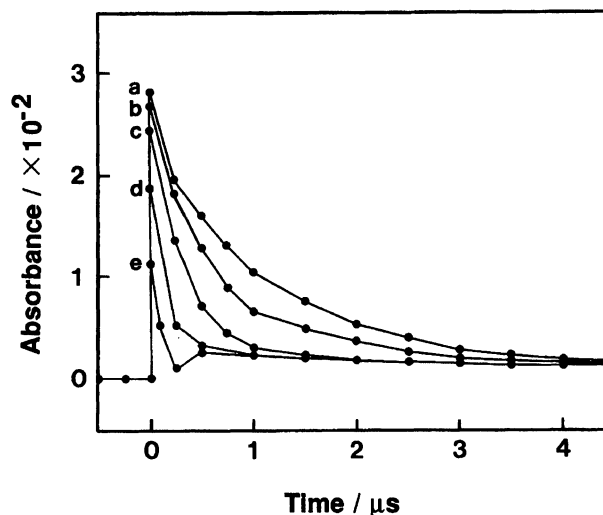


Fig. 5. Quenching patterns of transient absorption of hydrated electrons with nitrate (seawater from station A). The concentrations of nitrate are (a) 0.00, (b) 0.05, (c) 0.10, (d) 0.40, and (e) 1.00 mmol L<sup>-1</sup>. Each dot represents the mean value for three measurements.

Table 2. The Calculated Rate Constants ( $k$ ,  $k_p$ , and  $k_t$ ) from the Intensity and Lifetime of the Hydrated Electrons

St. A			
Quencher	$k/\text{L mol}^{-1} \text{s}^{-1}$ <sup>a)</sup>	$k_p/\text{L mol}^{-1} \text{s}^{-1}$ <sup>b)</sup>	$k_t/\text{L mol}^{-1} \text{s}^{-1}$ <sup>c)</sup>
Nitrite	$8.4 \pm 0.3 \times 10^9$	$9.4 \pm 0.3 \times 10^8$	$8.3 \pm 0.4 \times 10^9$
Nitrate	$1.0 \pm 0.3 \times 10^{10}$	$1.0 \pm 0.3 \times 10^9$	$1.0 \pm 0.2 \times 10^{10}$
Cd <sup>2+</sup>	$1.3 \pm 0.3 \times 10^{10}$	$7.4 \pm 0.2 \times 10^8$	$1.2 \pm 0.5 \times 10^{10}$
Ni <sup>2+</sup>	$3.1 \pm 0.3 \times 10^9$	$1.5 \pm 0.1 \times 10^8$	$3.1 \pm 0.3 \times 10^9$
Co <sup>2+</sup>	$1.9 \pm 0.3 \times 10^9$	$8.2 \pm 0.5 \times 10^7$	$1.9 \pm 0.1 \times 10^9$
[Co(NH <sub>3</sub> ) <sub>6</sub> ] <sup>3+</sup>	$3.4 \pm 0.3 \times 10^{10}$	$2.5 \pm 0.6 \times 10^9$	$3.5 \pm 0.3 \times 10^{10}$
St. B			
Quencher	$k/\text{L mol}^{-1} \text{s}^{-1}$	$k_p/\text{L mol}^{-1} \text{s}^{-1}$	$k_t/\text{L mol}^{-1} \text{s}^{-1}$
Nitrite	$8.1 \pm 0.3 \times 10^9$	$4.4 \pm 0.1 \times 10^8$	$8.1 \pm 0.1 \times 10^9$
Nitrate	$1.3 \pm 0.3 \times 10^{10}$	$2.9 \pm 0.3 \times 10^8$	$1.3 \pm 0.3 \times 10^{10}$
Cd <sup>2+</sup>	$1.1 \pm 0.3 \times 10^{10}$	$7.3 \pm 0.2 \times 10^8$	$1.1 \pm 0.4 \times 10^{10}$
Ni <sup>2+</sup>	$4.5 \pm 0.3 \times 10^9$	$1.9 \pm 0.5 \times 10^8$	$4.5 \pm 0.5 \times 10^9$
Co <sup>2+</sup>	$2.4 \pm 0.3 \times 10^9$	$8.1 \pm 0.3 \times 10^7$	$2.2 \pm 0.1 \times 10^9$
St. C at 18:00			
Quencher	$k/\text{L mol}^{-1} \text{s}^{-1}$	$k_p/\text{L mol}^{-1} \text{s}^{-1}$	$k_t/\text{L mol}^{-1} \text{s}^{-1}$
Nitrite	$7.9 \pm 0.3 \times 10^9$	$7.8 \pm 0.3 \times 10^8$	$7.9 \pm 0.2 \times 10^9$
Nitrate	$9.4 \pm 0.3 \times 10^9$	$9.9 \pm 0.1 \times 10^8$	$9.0 \pm 0.5 \times 10^9$
Cd <sup>2+</sup>	$9.4 \pm 0.3 \times 10^9$	$8.2 \pm 0.4 \times 10^8$	$9.4 \pm 0.4 \times 10^9$
Ni <sup>2+</sup>	$4.5 \pm 0.3 \times 10^9$	$1.2 \pm 0.1 \times 10^8$	$4.5 \pm 0.3 \times 10^9$
Co <sup>2+</sup>	$1.7 \pm 0.3 \times 10^9$	$9.3 \pm 0.3 \times 10^7$	$1.7 \pm 0.2 \times 10^9$

a) From  $[E]=e^{-k[Q]t}$ . b) From  $k_p=K_{SV}^p/\tau_0$ . c) From  $k_t=K_{SV}^t/\tau_0$ .

was given as:

$$I_0/I = 1 + K_{SV}^p[Q] = 1 + k_p\tau_0[Q] \quad (4)$$

$K_{SV}^p$  and  $k_p$  are the quenching constant for absorption intensity and the quenching rate constant for absorption intensity, respectively. The values of  $k_p$  were smaller than those of  $k$  and  $k_t$  (Fig. 7 and Table 2). The values

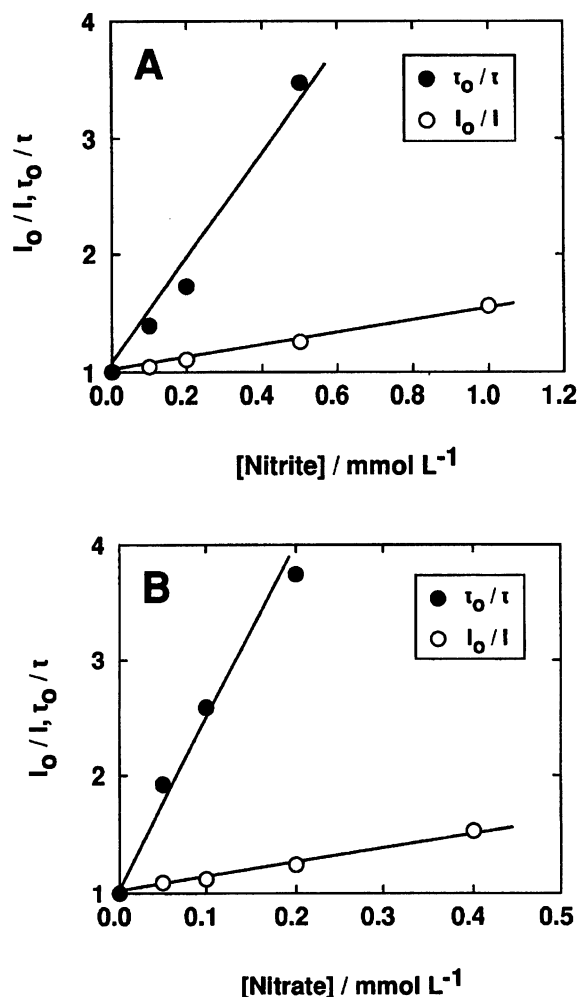


Fig. 6. Stern-Volmer plots for the absorption intensity and the lifetime of hydrated electrons in seawater from station A. Quencher: (A) nitrite, (B) nitrate.

of  $k_p$  seem to reflect primary quenching of the hydrated electrons generated, caused by the quenchers associated with the DOM (photosensitizer) in the samples. In this process, quenching occurs before diffusion or at the start of diffusion of the hydrated electrons from the DOM. The values of  $k_p$  being smaller than  $k$  and  $k_t$  can be explained by the limited number of sites in DOM for association with the quencher.

Figure 8 shows Stern-Volmer plots of  $I_0/I$  vs. the nitrite or nitrate concentration for samples from stations A, B, and C at 18:00. With either nitrite or nitrate, the slope of the lines of regression ( $K_{SV}^P = k_p \cdot \tau_0$ ) of the sample from station B was smaller than that of the samples from stations A or C. If the value of  $k_p$  is related to the magnitude of the association between the quencher and the DOM, the small  $k_p$  of the sample from station B implies that the DOM in the sample is anionic. This regional difference was not seen in quenching by metal ions. The similarity of the values of  $k_p$ , obtained the study of quenching by the metal ions, can be explained by the seawater already containing cations (most likely

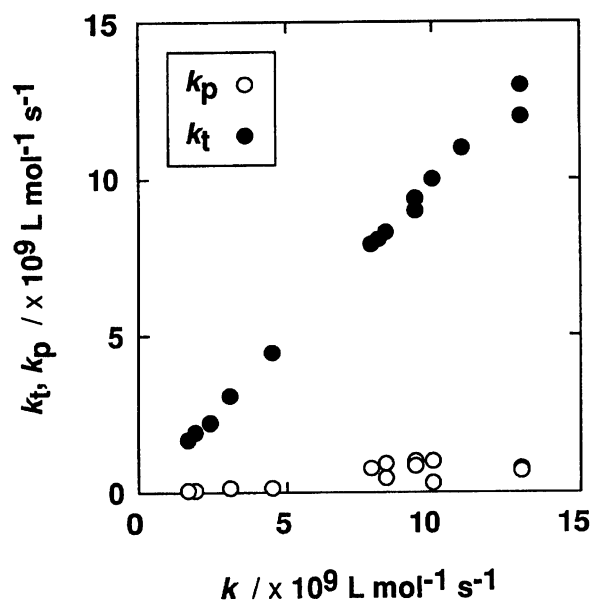


Fig. 7. Correlation between quenching rate constants  $k$ ,  $k_p$  (open circles), and  $k_t$  (closed circles).

$\text{Mg}^{2+}$  and  $\text{Ca}^{2+}$ ). These ions act as counterions and reduce the association between the DOM and the added cationic quenchers.  $\text{Mg}^{2+}$  and  $\text{Ca}^{2+}$  affect the interaction of these ions and fluorescent DOM in estuary waters.<sup>31)</sup>

Figure 9 shows Stern-Volmer plots of  $I_0/I$  vs. nitrite and nitrate concentration for samples from Okuda Pond. The plots down curved as the concentrations of nitrate or nitrite increased, as was found in quenching in other land waters. There are at least two possible explanations for the downward curvature. First, the association between a quencher and DOM in land water is saturated when the concentration is high. Second, whether there is saturation or not, hydrated electrons from some fractions of the DOM are not accessible to the quencher. The second hypothesis implies that hydrated electrons generated in the interior of the DOM are not accessible to the quencher associated with the DOM, which is supported by DOM in land waters being an aggregate.<sup>4)</sup>

## Conclusions

Results presented here give additional evidence that absorption of near-UV light causes ejection of hydrated electrons from the DOM in natural waters. The DOM in land waters was rich in fluorescent organic matter and ejected more hydrated electrons than seawater DOM under the same conditions of laser photolysis. These results suggest that the DOM in land water contains photochemically sensitive chromophores more than that in seawater. When cations were used as the quencher, no regional difference in the quenching rate constant of hydrated electrons was found for coastal and open ocean seawaters, suggesting similar quenching mecha-

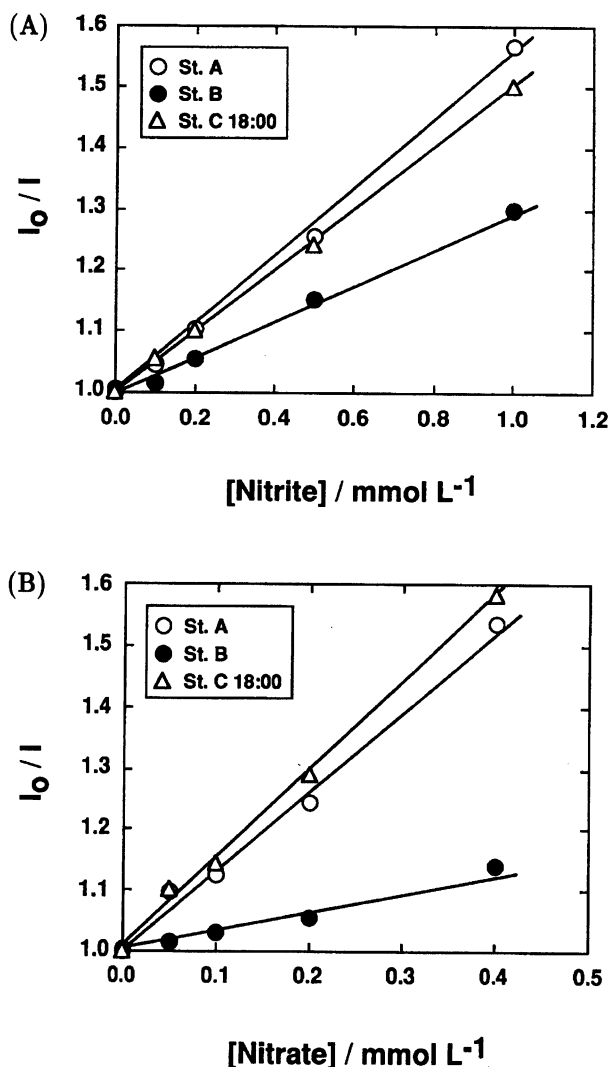


Fig. 8. Stern-Volmer plots of  $I_0/I$  vs. the nitrite or nitrate concentration for samples from stations A, B, and C at 18:00. Quencher: (A) nitrite, (B) nitrate.

nisms for hydrated electrons generated in the different seawaters. Quenching of hydrated electrons by anions showed a regional difference was caused by the variations in the stability of the quencher-DOM association. Quenching studies suggested that DOM was an aggregate in land waters. These observations of the quenching of hydrated electrons based on the Stern-Volmer model, which is conceptually simple, can be helpful to interpret the natural DOM properties as demonstrated in this work.

We thank Y. Kodama and H. Hasumoto for assistance with sampling and the crews of the research vessel Tansei Maru and Hakuhou Maru of the Ocean Research Institute, University of Tokyo, for their help during the research cruise. We thank T. Seiki, Hiroshima Prefectural Health and Environment Center, for his help with DOC measurements. This research was partially supported by Grants-in-Aid Nos. 02453033, 03248101, and

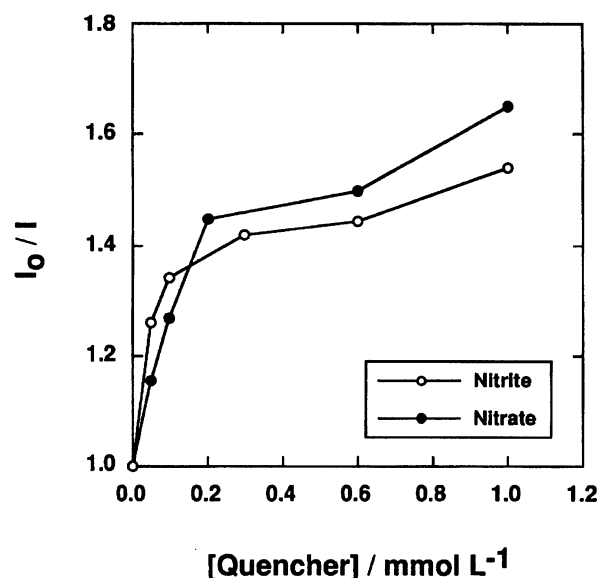


Fig. 9. Stern-Volmer plots of  $I_0/I$  vs. nitrite and nitrate concentration for samples from Okuda Pond. Quencher: nitrite (open circles), nitrate (closed circles).

04232101 from the Ministry of Education, Science and Culture.

#### References

- 1) A. A. M. Roof, "Handbook of Environmental Chemistry," ed by O. Hutzinger, Springer-Verlag, Berlin (1982), Vol. 2, Part B, p. 43.
- 2) O. C. Zafriou, J. Jousot-Dubien, R. G. Zepp, and R. G. Zika, *Environ. Sci. Technol.*, **18**, 358A (1984).
- 3) R. G. Zika, *Rev. Geophys.*, **25**, 1390 (1987).
- 4) G. G. Choudhry, "Handbook of Environmental Chemistry," ed by O. Hutzinger, Springer-Verlag, Berlin (1982), Vol. 2, Part B, p. 103.
- 5) R. G. Zepp, P. F. Schlotzhauer, and R. M. Sink, *Environ. Sci. Technol.*, **19**, 74 (1985).
- 6) J. A. Amador, P. J. Milne, C. A. Moore, and R. G. Zika, *Mar. Chem.*, **28**, 1 (1990).
- 7) A. M. Fisher, D. S. Kliger, J. S. Winterle, and T. Mill, *Chemosphere*, **14**, 1299 (1985).
- 8) A. M. Fisher, J. S. Winterle, and T. Mill, "Photochemistry of Environmental Aquatic Systems," ed by R. G. Zika and W. J. Cooper, American Chemical Society, Washington, DC (1987), ASC Symposium Series 327, p. 141.
- 9) F. H. Frimmel, H. Bauer, J. Putzien, P. Murasecco, and A. M. Braun, *Environ. Sci. Technol.*, **21**, 541 (1987).
- 10) J. F. Power, D. K. Shama, C. H. Langfor, R. Bonneau, and J. Jousot-Dubien, "Photochemistry of Environmental Aquatic Systems," ed by R. G. Zika and W. J. Cooper, American Chemical Society, Washington, DC (1987), ASC Symposium Series 327, p. 157.
- 11) R. G. Zepp, A. M. Braun, J. Hoigne, and J. A. Leenheer, *Environ. Sci. Technol.*, **21**, 485 (1987).
- 12) K. Fujiwara, T. Ushiroda, K. Takeda, Y. Kumamoto, and H. Tsubota, *Geochem. J.*, **27**, 103 (1993).
- 13) H. I. Joschek and L. I. Grossweiner, *J. Am. Chem.*

*Soc.*, **88**, 3261 (1966).

14) G. Grabner, G. Köler, J. Zeehner, and N. Getoff, *Photochem. Photobiol.*, **26**, 449 (1977).

15) W. J. Cooper and R. G. Zika, *Science*, **220**, 711 (1983).

16) R. G. Petasne and R. G. Zika, *Nature*, **325**, 516 (1987).

17) W. J. Cooper, R. G. Zika, R. G. Petasne, and J. M. C. Plane, *Environ. Sci. Technol.*, **22**, 1156 (1988).

18) R. F. Chen and J. L. Bada, *Mar. Chem.*, **37**, 191 (1992).

19) K. Kalle, *Dtsch. Hydrogr. Z.*, **2**, 9 (1949).

20) J. E. Dorsch and T. F. Bidleman, *Estuarine Coastal Shelf Sci.*, **15**, 701 (1982).

21) E. J. Hart and M. Anbar, "The Hydrated Electron," John Wiley & Sons, New York (1970).

22) C. J. W. Kramer, *Neth. J. Sea Res.*, **13**, 325 (1979).

23) W. C. Dunlap and M. Susic, *Mar. Chem.*, **19**, 99 (1986).

24) K. Hayase, M. Yamamoto, I. Nakazawa, and H. Tsubota, *Mar. Chem.*, **20**, 265 (1987).

25) K. Hayase, H. Tsubota, I. Sunada, S. Goda, and H. Yamazaki, *Mar. Chem.*, **25**, 373 (1988).

26) R. F. Chen and J. L. Bada, *Geophys. Res. Lett.*, **16**, 687 (1989).

27) P. L. Smart, B. L. Finlayson, W. D. Rylands, and C. M. Ball, *Water Res.*, **10**, 805 (1976).

28) R. W. P. M. Laane and L. Koole, *Neth. J. Sea Res.*, **15**, 217 (1982).

29) "Handbook of Chemistry and Physics," 60th ed, ed by R. C. Weast, C. R. C. Press, Boca Raton, Florida (1979), p. D155.

30) O. Stern and M. Volmer, *Physik. Z.*, **20**, 183 (1919).

31) J. D. Willey, *Mar. Chem.*, **15**, 59 (1984).

---